



Research Article

Design of reactive powder concrete mortar mixes through high strength and durability

Yousry B. I. Shaheen ^a , Zeinab A. Etman ^a , Hanan Lotfy Sabiha ^{b,*} 

^a Department of Civil Engineering, Menoufia University, 32511 Shebin ElKoum, Menoufia, Egypt

^b Higher Institute of Engineering and Technology, Menoufia University, 32511 Shebin ElKoum, Menoufia, Egypt

ABSTRACT

This research investigates the characteristics of reactive powder concrete (RPC) through comprehensive analysis. The primary methodology involved evaluating both fresh (uncured) and hardened RPC specimens. The initial phase incorporated silica fume (SF) as a cement replacement at concentrations of 5, 10, 15, 20, and 25%, fly ash (FA) substitution at levels of 5, 10, 20, 25, and 30% of the cement content, plus binary combinations where SF constituted 10% cement replacement while FA proportions ranged from 10 to 30%. Material behavior was assessed through slump flow testing procedures. Hardened concrete evaluation encompassed dry density measurements, compressive strength analysis conducted at 7, 28, 56, and 90-day intervals, along with tensile splitting strength and flexural strength determination at 28 days. Results demonstrate that FA substitution alone provides superior workability compared to SF+FA combinations and pure SF, whereas SF replacement individually exhibits enhanced compressive, tensile splitting, and flexural strength performance relative to standalone FA and binary SF+FA mixtures. The subsequent investigation phase examined the influence of nano-silica (NS) on fresh and hardened RPC characteristics. NS replaced cement at 1, 2, 3, 4, and 5% levels, combined with 10% SF and 20% FA. Findings revealed that increased NS content diminishes workability due to elevated water demand for hydration and mixing processes as particle fineness increases. Regarding hardened properties, the optimal composition comprises 10% SF, 20% FA, and 3% NS, attributed to NS's effective interaction with calcium hydroxide generated during cement hydration, which facilitates additional C-S-H formation through enhanced pozzolanic reactions. This mechanism results in improved mixture performance and strength development.

Citation: Shaheen YBI, Etman ZA, Sabiha HL (2025). Design of reactive powder concrete mortar mixes through high strength and durability. *Challenge Journal of Concrete Research Letters*, 16(3), 142–154.

1. Introduction

Reactive powder concrete (RPC) belongs to the group of ultrahigh-performance concretes. All the components in RPC are chemically active, which is why it is referred to as reactive powder. Several studies have found that ultra high performance concrete (UHPC) is not considered concrete because it is not made with coarse aggregate (Sadrekarimi 2004). The word “concrete” is used for ultrahigh-performance concrete because it contains

steel fibers to make it stronger and more flexible (Aitcin 2000). On the other hand, RPC development does not require fibers. RPC was created by applying microstructural modification techniques, which changed its characteristics, including remarkable durability, high compressive strength, and toughness (Richard and Cheyrezy 1995). Currently, specific methods and raw materials need to be used in RPC production in order to obtain outstanding mechanical performance. These include (Sarika and Elson 2015):

ARTICLE INFO

Article history:

Received – January 1, 2025
Revision requested – March 25, 2025
Revision received – June 2, 2025
Accepted – June 25, 2025

Keywords:

Reactive powder concrete
Blast furnace slag cement
Silica fume
Fly ash
Nano silica



This is an open access article distributed under the CC BY licence.

© 2025 by the Authors.

* Corresponding author. E-mail address: hanan_lotfy85@yahoo.com (H. L. Sabiha)

- Removing coarse aggregate from the concrete to increase homogeneity.
- Making composite materials more ductile by adding steel tubes or metal fibers.
- Using large quantities of quartz and premium superplasticizer to create a low water/binder ratio, which reduces porosity and increases strength.
- Applying pressure both prior to and during the setting process to increase compactness.
- Utilizing cementitious materials containing highly active micro-silica and/or precipitated silica to accelerate cement hydration and catalyze a strong pozzolanic reaction.
- Applying steam curing to achieve greater strength.

To develop UHPC that achieves target strength performance, carefully selected raw materials and advanced processing methods are necessary. In recent years, multiple researchers have studied RPC characteristics and behavior. Numerous successful RPC applications include the Sherbrooke Bridge in Canada (60-meter span), the Future Bridge in the United States (25-meter length), seawall anchor systems in Portugal, various automotive bridges in Australia, and the manufacture of structural beam elements, manhole covers, roadway accessories, and other products. Presently, extensive research is conducted on RPC to investigate its response and behavior.

Silica fume (SF), a supplementary cementitious material (SCM), is a byproduct of silicon and ferrosilicon manufacturing. It appears in powder form as spherical particles approximately 200 nm in diameter. Since less cement is used in the composition, SF enhances hardened concrete properties while promoting environmental compatibility. SF addition has been associated with increased C-S-H gel formation and reduced $\text{Ca}(\text{OH})_2$ content, which significantly improves matrix microstructural density and reduces porosity (Chandra and Berntson 1996; Aitcin 2016; Kurdowski 2014; Ullah et al. 2022). SF substantially improves the mechanical characteristics of RPC. It increases RPC packing density and enhances the interfacial transition zone between paste and aggregate. Compared to SCM formulations using fly ash (FA) or ground granulated blast-furnace slag, the primary limitation of RPC compositions with SF is reduced workability at higher SF contents (Bahmani and Mostofinejad 2022; Ge et al. 2023; Ju et al. 2017; Shen et al. 2022; Sultan et al. 2022).

Using 20% FA as a partial cement replacement modifies the ITZ microstructure and enhances mechanical properties to some degree, particularly under elevated temperatures and autoclave pressure. FA requires less water for reactions compared to SF (Golewski 2018; Hefni et al. 2018; Moffatt et al. 2017; Yazıcı et al. 2009; Yu et al. 2015).

The integration of nanoparticles into concrete is gaining recognition for its beneficial effects on fresh and hardened properties, attributed to their unique surface area characteristics. The most common nanoparticles used in concrete to enhance the cement matrix include nano-alumina, nano-titania, nano-iron oxide, nano-silica (NS), nano-zinc oxide, and nano-clay. Among these, NS, a conventional inorganic non-metallic oxide nanomaterial with high specific surface area and reactivity, is consid-

ered the most suitable nanoparticle for concrete applications (Rashad 2014). Through pozzolanic mechanisms, NS has been shown to improve the mechanical properties of cement-based materials (Balapour et al. 2018; Kong et al. 2012; Zhang et al. 2016). It has been concluded that the early compressive strength of high-performance concrete is more significantly affected by NS incorporation compared to later strength development. Furthermore, optimal mixing proportions are suggested to range between 3% and 5% NS (Wang 2011).

RPC compressive strength, flexural strength, and impact resistance all increase when the water-cement ratio is reduced, as this leads to greater density and lower porosity. The specimen with the highest overall mechanical performance had a 0.16 water-cement ratio, 134.4 MPa compressive strength, 16.86 MPa flexural strength, and the ability to withstand 1,150 destructive impacts (Tan et al. 2025).

Albakry and Abbas (2025) examined the influence of four different curing methods on RPC mechanical properties. The most substantial improvements in mechanical strength (compressive, flexural, and splitting tensile) were achieved in the Steam + Normal Curing (R-S) system, particularly with 1–3 day curing durations, followed by Normal Curing (R-N) at 28 and 90 days.

RPC offers exceptional strength and durability, making it ideal for constructing large-span lightweight structures and those required to withstand severe weather conditions, thus improving infrastructure longevity and reliability. The implementation of RPC aligns with sustainable development objectives by reducing the demand for natural resources, extending the service life of structures, and decreasing waste production, thereby fostering eco-friendly practices within the construction sector (Zhao 2024).

2. Material Properties

The materials used in this research to produce local RPC mixes were blast furnace slag cement, SF, FA, sand, NS, polypropylene fiber, superplasticizers, and water, as shown in Fig. 1.

2.1. Blast furnace slag cement

The research used blast furnace slag cement (CEM III/A 42.5 N) with a specific gravity of 2.9, according to E.S.S. 4756-1 (2013). Its main properties are shown in Tables 1 and 2.

2.2. Silica fume

Silica fume was used as a pozzolanic material meeting the requirements of E.S.S. 5129-1 (2006). Tables 3 and 4 show the chemical and physical properties of silica fume.

2.3. Fly ash

Fly ash Class F was used as a pozzolanic material meeting the requirements of ASTM C618 (2019). Tables 5 and 6 show the chemical and physical properties of fly ash.

Table 1. Mechanical and physical properties of the cement used.

| Property | | Value | Limits |
|---|-----------------------|--------------------------|--|
| Specific gravity | | 2.9 | -- |
| Setting time | Initial (min) | 60 | Not less than 45 min |
| | Final (hrs) | 5.25 | Not more than 10 hrs |
| | Fineness | 3733 cm ² /gm | Not less than 2500 cm ² /gm |
| | Soundness (expansion) | 1 | Not more than 10 mm |
| Compressive strength (N/mm ²) | 2 days | 12.96 | -- |
| | 7 days | 27.33 | -- |
| | 28 days | 47.74 | -- |

Table 2. Chemical properties of the cement used.

| Oxides | Value % | % max |
|--------------------------------|---------|-------|
| SiO ₂ | 23.63 | -- |
| Al ₂ O ₃ | 9.07 | -- |
| Fe ₂ O ₃ | 3.45 | -- |
| CaO | 51.54 | -- |
| MgO | 4.66 | -- |
| SO ₃ | 2.71 | 4.0 |
| K ₂ O | 0.35 | -- |
| Cl | 0.03 | 0.1 |
| Na ₂ O | 0.34 | -- |
| (IR) Insoluble residue | 2.09 | 5.0 |
| (LOI) Loss on ignition | 2.02 | 5.0 |
| Equivalent Alkalis | 0.58 | -- |

Table 3. Chemical composition of silica fume.

| Chemical composition | Mass, % |
|--------------------------------|-----------|
| SiO ₂ | 92-94 |
| Al ₂ O ₃ | 0.2-0.3 |
| Fe ₂ O ₃ | 0.1- 0.5 |
| CaO | 0.1- 0.15 |
| MgO | 0.1-0.2 |
| Na ₂ O | 0.1 |
| K ₂ O | 0.1 |
| Carbon | 3-5 |
| MnO | 0.008 |

Table 4. Physical properties of silica fume.

| | |
|-----------------------------|----------------------------|
| Moisture content, % | 0.5 max |
| Size above 45 μm | |
| Specific gravity | 2.13 |
| (BET) Particle Surface Area | 15.0 m ² /g min |

Table 5. Chemical composition of fly ash.

| Chemical composition | Mass, % |
|--------------------------------|---------|
| SiO ₂ | 55.71 |
| Al ₂ O ₃ | 22.56 |
| Fe ₂ O ₃ | 5.61 |
| Sum | 83.88 |
| MgO | 10.44 |
| SO ₃ | 1.78 |
| Na ₂ O | 0.54 |
| K ₂ O | 0.79 |
| Total alkalis | 0.76 |
| Available alkalis | 0.26 |
| Loss on ignition (LOI) | 0.41 |

Table 6. Physical properties of fly ash.

| | |
|--|-------|
| Moisture content, % | 0.16 |
| Amount retained on No. 325 sieve, % | 23.63 |
| Specific gravity | 2.2 |
| <u>Autoclave soundness, %</u> | |
| Strength activity index with portland cement at 7days, % of control | 77.1 |
| Strength activity index with portland cement at 28days, % of control | 85.5 |
| Water required, % of control | 94.6 |

2.4. Sand

According to E.S.S. 1109 (2008), fine aggregate was used to produce the mortar specimens in this study. The particle size of the quartz sand used for producing RPC ranged from 150 to 650 μm, with a specific gravity of 2.65.

2.5. Nano-silica

Nano-silica (NS) served as a concrete additive for enhancing cement hydration processes, improving durability characteristics, and optimizing the mechanical behavior of both fresh and hardened concrete. The chemical characteristics of NS are presented in Table 7.

Technical specifications include:

- Elevated purity levels ranging from 96.7% to 99%
- Completely natural sand composition (100%)
- Moisture-free sand with no water content
- Superior particle size gradation
- Spherical grain morphology
- Absence of organic matter and contaminants
- Non-radioactive material
- Non-hazardous composition
- Turbidity measurements below 100 units
- Dust-free condition
- Absence of heavy metals

2.6. Polypropylene fiber

Fibers were graded in lengths of 6, 12, and 20 mm, with an average diameter of 0.034 mm. They had a tensile strength of 500–700 MPa, a density of 900 kg/m³, a melting point of 162 °C, a modulus of elasticity of 2800 MPa, and an elongation of 25%, according to ASTM C1116 (2010) and ASTM C1339 (2008).

2.7. Superplasticizer

As a superplasticizer, a high-range water-reducing admixture (HRWRA), according to ASTM C1017 (2013) (Type A and F), was used. The admixture is brown and weighs 1.18 kg per liter at room temperature. The

amount of HRWRA was 2% of the total binder weight (fly ash, cement, silica fume, and nano-silica).

2.8. Water

No impurities were allowed in the potable water used for making and curing the concrete. The water-to-binder ratio (silica fume + fly ash + cement + nano-silica) was set at 0.23.

Table 7. Chemical properties of nano-silica.

| Oxides | % min | % max |
|--------------------------------|-------|-------|
| SiO ₂ | 99.4 | 99.4 |
| Al ₂ O ₃ | 0.06 | 0.09 |
| Na ₂ O | 0.05 | 0.07 |
| K ₂ O | 0.01 | 0.02 |
| CaO | 0.02 | 0.09 |
| MgO | 0.03 | 0.03 |
| Fe ₂ O ₃ | 0.012 | 0.018 |
| TiO ₂ | 0.017 | 0.021 |
| Cr ₂ O ₃ | 2 ppm | 2 ppm |
| L.O.I. | 0.15 | 0.25 |



Fig. 1. Materials: Silica fume; Fly ash; Nano-silica; Polypropylene Fiber300–e3; Super-plasticizer.

3. Casting and Mix Proportion

Four RPC groups comprising 21 mixtures were examined to meet the study's objectives, as indicated in Table 8. With a cementitious content of 990.3 kg/m³, the first group (SF) included mixes M01 to M05, in which SF partially replaced cement at 5, 10, 15, 20, and 25%. The second group (FA), also with a cementitious content of 990.3 kg/m³, consisted of mixes M06 to M11, where FA partially replaced cement at 5, 10, 15, 20, 25, and 30%. The third group (SF+FA), with the same cementitious content, consisted of mixes M12 to M16, incorporating 10% SF and partial FA replacement at 10, 15, 20, 25, and 30%. The fourth group (SF+FA+NS) also had a cementitious content of 990.3 kg/m³ and included mixes M17 to M21, containing 10% SF, 20% FA, and partial NS replacement at 1, 2, 3, 4, and 5%.

All mixes were cured in ordinary water at 25 °C. To prepare the mixtures, the sand and fine materials were blended in a mixer for two minutes. Water and superplasticizer were then added, and mixing continued for seven minutes until a uniform consistency was achieved.

Polypropylene fiber was added next, and the mixture was blended for an additional five minutes to ensure homogeneity. An electric hand mixer was used to finalize the mix. The concrete was then poured into molds to create the specimens.

Specimens were demolded 24 hours after casting and cured in water at approximately 25 °C. At the time of testing, the specimens were removed from the water. To ensure consistent curing conditions, all specimens were treated in the same curing tanks.

4. Testing Method

Mechanical property evaluations were conducted using standard specimens in accordance with ASTM C109 (2020) for compressive strength, ASTM C348 (2021) for flexural strength, and ASTM C496 (2017) for splitting tensile strength. Strength assessments utilized cubic specimens (70×70×70 mm), cylindrical specimens (50×100 mm), and prismatic specimens (40×40×160 mm).

Table 8. Constituents of concrete mixes (kg/m³) (sand/cement=1.1; water/binder=23%).

| Group | Mix No. | Cement (kg/m ³) | Sand (kg/m ³) | Water (kg/m ³) | HRWRA (kg/m ³) | PPF (kg/m ³) | SF (kg/m ³) | FA (kg/m ³) | SiO ₂ (kg/m ³) |
|--|----------------------------|-----------------------------|---------------------------|----------------------------|----------------------------|--------------------------|-------------------------|-------------------------|---------------------------------------|
| - | Control | 990.20 | 1089.2 | 227.75 | 19.8 | 2.7(0.3%)* | -- | -- | -- |
| Silica fume (SF) | M01 (5%) | 940.69 | | | | | 49.51 | -- | -- |
| | M02 (10%) | 891.18 | | | | | 99.02 | -- | -- |
| | M03 (15%) | 841.67 | 1089.2 | 227.75 | 19.8 | 2.7(0.3%)* | 148.53 | -- | -- |
| | M04 (20%) | 792.16 | | | | | 198.04 | -- | -- |
| | M05 (25%) | 742.65 | | | | | 247.55 | -- | -- |
| Fly Ash (FA) | M06 (5%) | 940.69 | | | | | -- | 49.51 | -- |
| | M07 (10%) | 891.18 | | | | | -- | 99.02 | -- |
| | M08 (15%) | 841.67 | 1089.2 | 227.75 | 19.8 | 2.7(0.3%)* | -- | 148.53 | -- |
| | M09 (20%) | 792.16 | | | | | -- | 198.04 | -- |
| | M10 (25%) | 742.65 | | | | | -- | 247.55 | -- |
| | M11 (30%) | 693.14 | | | | | -- | 297.06 | -- |
| Silica fume + Fly Ash (SF) + (FA) | M12 (10%SF + 10%FA) | 792.16 | | | | | 99.02 | 99.02 | -- |
| | M13 (10%SF + 15%FA) | 742.65 | | | | | 99.02 | 148.53 | -- |
| | M14 (10%SF + 20%FA) | 693.14 | 1089.2 | 227.75 | 19.8 | 2.7(0.3%)* | 99.02 | 198.04 | -- |
| | M15 (10%SF + 25%FA) | 643.63 | | | | | 99.02 | 247.55 | -- |
| | M16 (10%SF + 30%FA) | 594.12 | | | | | 99.02 | 297.06 | -- |
| Silica fume + Fly Ash + Nano-Silica (SF) + (FA) + (NS) | M17 (10%SF + 20%FA + 1%NS) | 683.24 | | | | | | | 9.90 |
| | M18 (10%SF + 20%FA + 2%NS) | 673.47 | | | | | | | 19.80 |
| | M19 (10%SF + 20%FA + 3%NS) | 663.43 | 1089.2 | 227.75 | 19.8 | 2.7(0.3%)* | 99.02 | 198.04 | 29.71 |
| | M20 (10%SF + 20%FA + 4%NS) | 653.53 | | | | | | | 39.61 |
| | M21 (10%SF + 20%FA + 5%NS) | 643.63 | | | | | | | 49.51 |

P.P: Poly Propylene; (*): Fiber volume fraction

4.1. Flow diameter assessment

Flow testing procedures were carried out for each mixture composition. Through flow diameter determination protocols, the values shown in Fig. 2(a) were obtained. The results demonstrate that reactive powder concrete exhibits satisfactory workability characteristics.

4.2. Compressive strength test

Compressive strength was evaluated using 70 mm cubic specimens at 7, 28, 56, and 90 days, as illustrated in Fig. 2(b).

4.3. Flexural strength test

Flexural strength was determined at 28 days using 40×40×160 mm prismatic specimens, as shown in Fig. 2(c).

4.4. Splitting tensile strength test

Splitting tensile strength was measured using cylindrical specimens measuring 50×100 mm at 28 days, as presented in Fig. 2(d).

4.5. Density

Density measurements were conducted on three 70 mm cubic specimens. According to ASTM C642 (2013), density is defined as the ratio of concrete mass to its corresponding volume. Dry density was evaluated at 28 days.

5. Results and Discussion

Several conditions were used to evaluate the characteristics of RPC. The following sections detail the outcomes of the experimental program.

5.1. Workability of RPC

The slump test was used to measure the fresh RPC properties for all mixes, considering the variety of binder materials (SF, FA, and NS) used at different ratios. The results are shown in Fig. 3. The flow diameter of the concrete decreases as the dosages of SF, FA, and NS increase. RPC mixes containing NS exhibit lower flowability than mixes containing only SF. This is explained by the fact that NS has a large surface area and requires more water to mix and flow properly (Ranjan et al. 2024).

RPC mixes containing FA show higher spread values than those containing SF. This is because excessive SF may reduce workability and increase fracture sensitivity, whereas FA improves fluidity without substantially affecting mechanical properties (Zhang et al. 2022). However, excessive fluidity may lead to concrete segregation.

Therefore, when using FA, it is advisable to lower the dosage of superplasticizer. The surface area of cementitious materials increases with fineness, necessitating more water for hydration and workability. Chemical admixtures must be used in varying amounts depending on the type and proportion of cementitious materials.



Fig. 2. Testing: Slump flow test; Compressive strength test; Flexural strength test; Splitting tensile strength test.

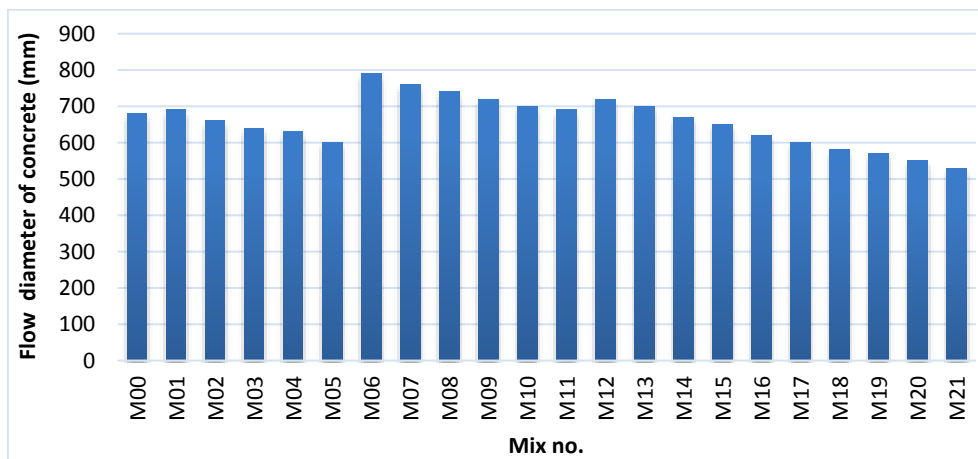


Fig. 3. The relation between the flow diameter of concrete and mix code for different mixes.

5.2. Compressive strength of RPC

5.2.1. Effect of the silica fume content

It was observed that silica fume improves the compressive strength of reactive powder concrete, with the optimal replacement level at 25%, as shown in Fig. 4. For mix M05, the compressive strength increased by 56.37% at 7 days, 57.5% at 28 days, 59.09% at 56 days, and 60.16% at 90 days compared to the control mix M00 at the same ages. This improvement is attributed to the enhanced hydration and densification of the RPC matrix due to the extremely fine silica fume particles, which increase its strength (Danha et al. 2013). In addition, silica fume particles react effectively with calcium hydroxide, reducing small particles and microcracks, and strengthening the microstructure.

Because silica fume is extremely fine, calcium hydroxide is able to form nuclei on its surface, which accelerates cement hydration. Silica fume also provides physical improvements by enabling particles to pack more closely, thereby strengthening the RPC matrix, making it denser, and enhancing the adhesion between cement and fibers (Neville 2005).

5.2.2. Effect of the fly ash content

The results demonstrate that incorporating 20% fly ash into reactive powder concrete enhances compressive strength performance, as shown in Fig. 5. At testing intervals of 7, 28, 56, and 90 days, mixture M09 exhibited compressive strength improvements of 35.52%, 36.47%, 36.89%, and 37.42%, respectively, compared to the control mixture M00 at the corresponding ages. The pozzolanic activity of fly ash facilitates reactions involving SiO_2 , Al_2O_3 , calcium hydroxide, and calcium silicate hydrate formation, resulting in enhanced density with reduced porosity and, consequently, improved concrete strength (Malheiro et al. 2020), alongside improved particle packing efficiency. The micro-filler capability of fly ash within cement paste voids contributes to increased density and subsequent strength enhancement.

Fig. 6 reveals that increasing fly ash content from 10% through 15%, 20%, 25%, to 30%, while maintaining a constant 10% silica fume content, produced minimal impact on 28-day compressive strength development. Substituting silica fume with fly ash in RPC offers economic benefits but affects compressive strength performance.

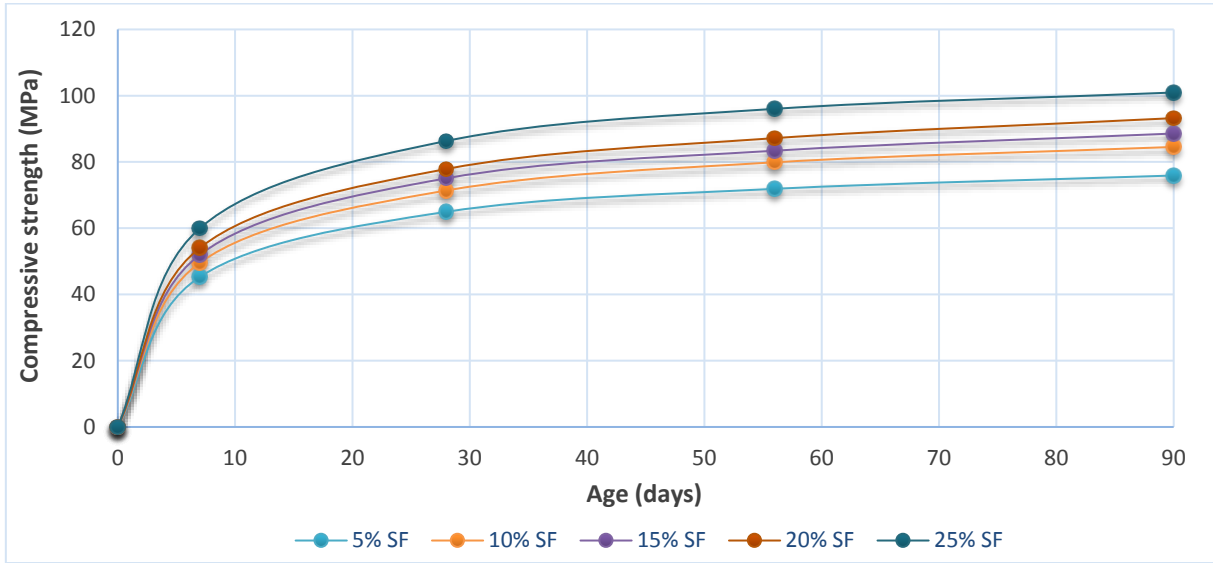


Fig. 4. Compressive strength of RPC using different ratios of silica fume.

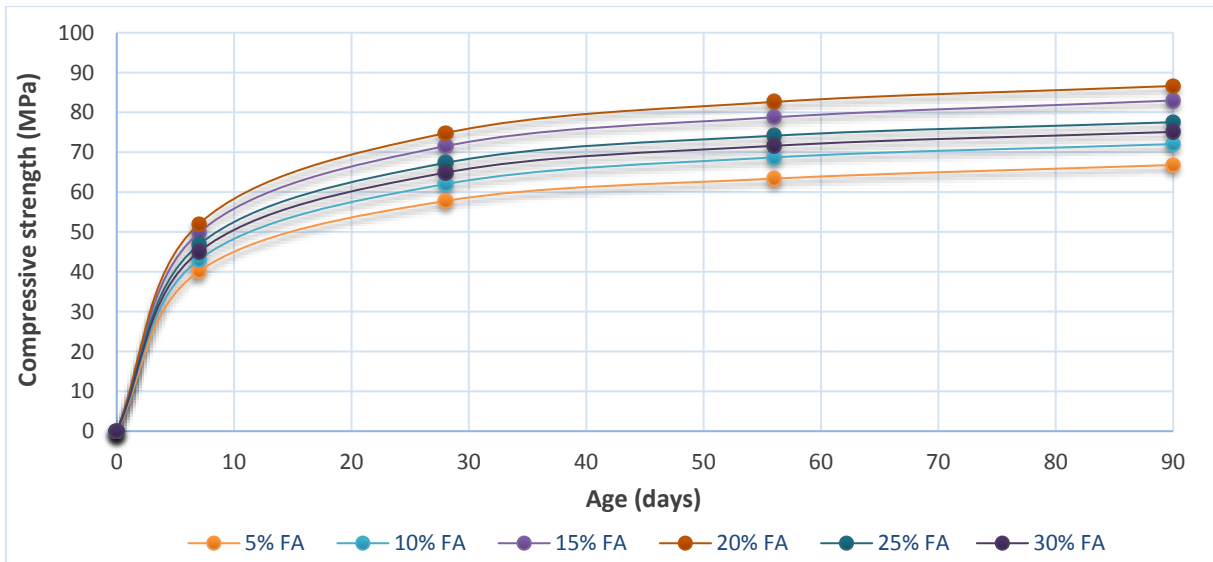


Fig. 5. Compressive strength of RPC using different ratios of fly ash.

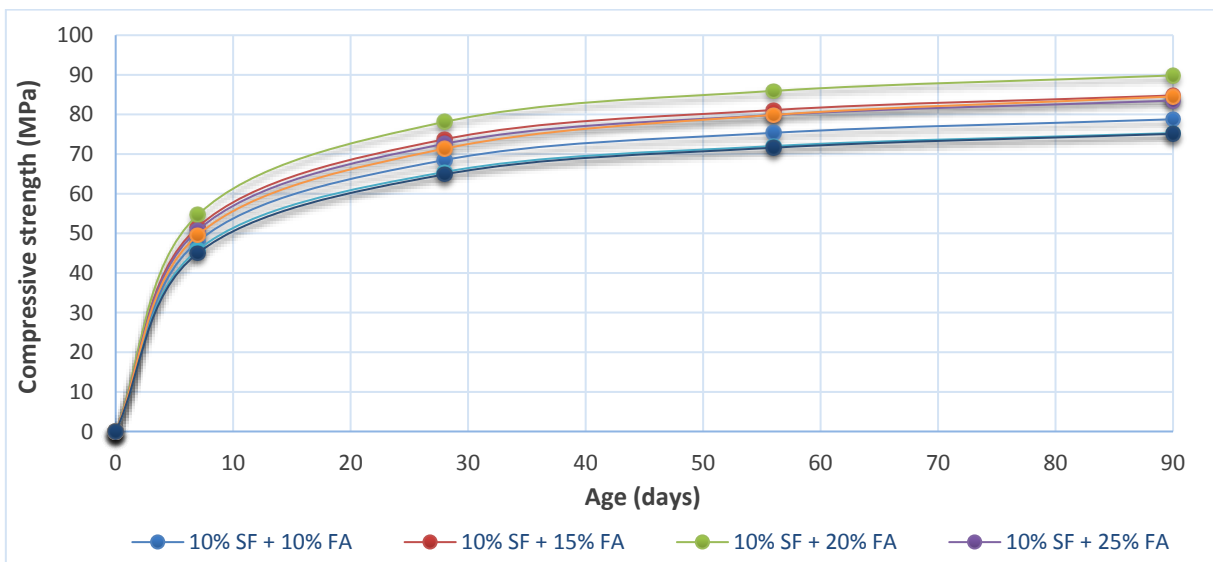


Fig. 6. Compressive strength of RPC using 10% silica fume with different ratios of fly ash.

The findings indicate that 30% fly ash replacement without silica fume achieved a 28-day compressive strength of 64.88 MPa, representing 16.96% lower performance compared to silica fume–fly ash combinations (10% SF + 20% FA). At equivalent ages and identical silica fume–fly ash proportions, silica fume demonstrated superior effectiveness in enhancing compressive strength.

Specifically, compressive strength improvements of 12.88%, 15.27%, 4.42%, 4.00%, and 28.20% were observed at 7 days, as shown in Fig. 7(a), with corresponding improvements of 12.41%, 15.11%, 4.92%, 4.10%, and 28.20% at 28 days, as illustrated in Fig. 7(b). In addition, Fig. 7(c) and Fig. 7(d) provides the compressive strength alteration at 56 days and 90 days, respectively.

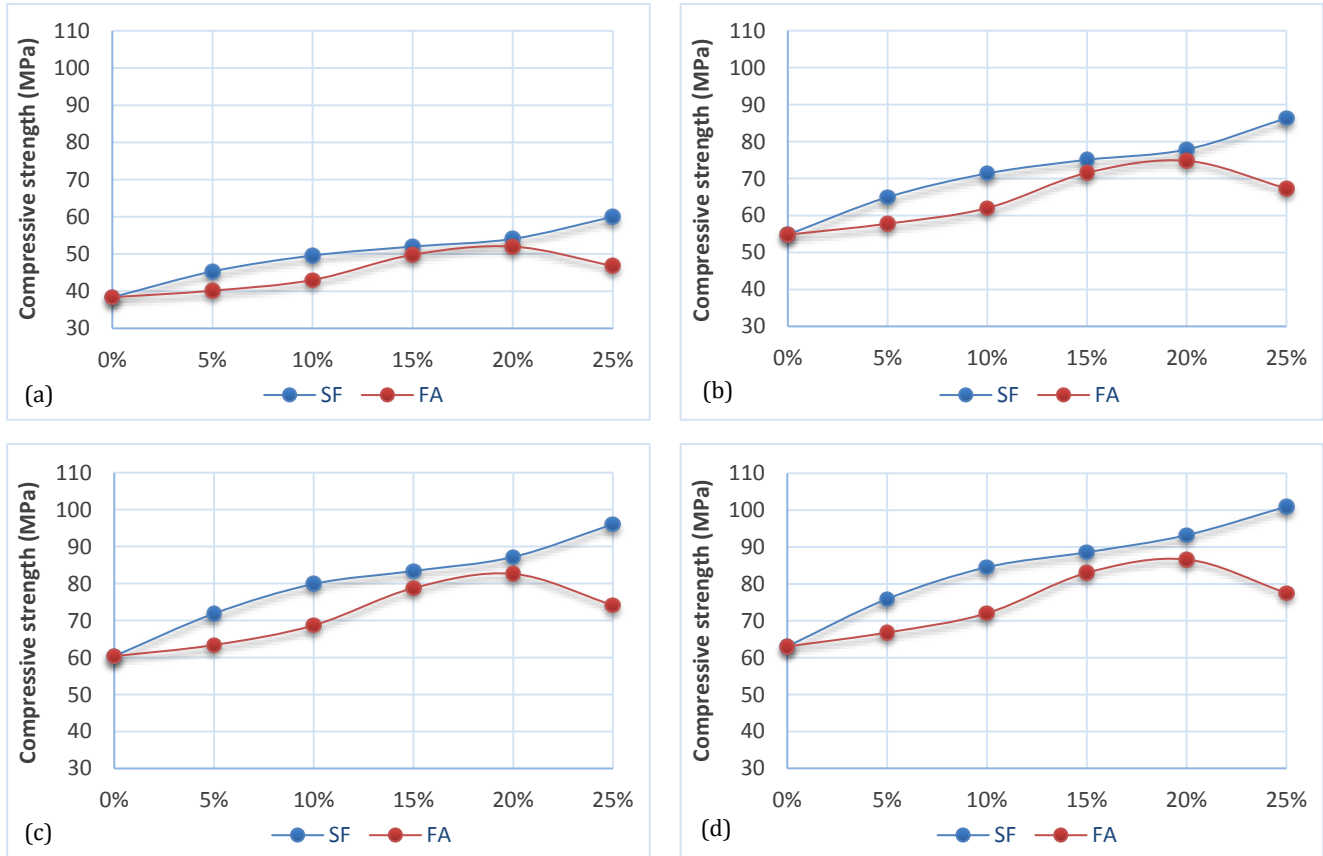


Fig. 7. Comparison between SF & FA at the same content: (a) at 7 days; (b) at 28 days; (c) at 56 days; (d) at 90 days.

5.2.3. Effect of the nano-silica content

Fig. 8 shows that nano-silica contents of 1%, 2%, 3%, 4%, and 5% were used together with 10% SF and 20% FA. The effect of this parameter on hardened concrete can be observed by examining mixes M17, M18, M19, M20, and M21. A maximum compressive strength of 103.13 MPa was recorded when 3% nano-silica was used. This was attributed to the optimal particle packing and the avoidance of strength reduction caused by particle agglomeration.

Nano-silica improved performance because it reacts with calcium hydroxide (CH) formed during cement hydration, producing additional calcium silicate hydrate (C-S-H) and strengthening the paste. With a stronger pozzolanic reaction, more C-S-H is generated, leading to greater overall strength (Rupasinghe et al. 2017). Nano-silica also enhances RPC by filling small pores and accelerating the formation of microstructural components that strengthen the concrete. As a result, the microstructure becomes denser, and the overall matrix strength increases (Ranjan et al. 2024).

5.3. Flexural strength of RPC

5.3.1. Effect of the silica fume content

Fig. 9 shows the flexural strength at 28 days for various rapid hardening portland (RHP) cement mixes containing silica fume at 5%, 10%, 15%, 20%, and 25%. By examining mixes M01, M02, M03, M04, and M05, the effect of silica fume content on results can be observed. Increasing the silica fume content from 5% to 25% of the binder improved the flexural strength of RPC by 11.72%, 30.45%, 52.95%, 63.64%, and 76.48%, respectively, compared to the control mix M00.

Based on the test results, the optimal silica fume content was found to be 25%, as shown in Fig. 9. This improvement is attributed to the extremely fine silica fume particles, which facilitate hydration and densification of the RPC matrix, thereby enhancing its strength.

5.3.2. Effect of the fly ash content

Fig. 10 illustrates the flexural strength performance of RPC mixtures incorporating fly ash at concentra-

tions of 5%, 10%, 15%, 20%, 25%, and 30% at 28-day maturity. Progressive fly ash incorporation demonstrates an overall enhancement in flexural strength,

with the maximum improvement of 49.10% observed at 20% fly ash replacement relative to the reference mixture M00.

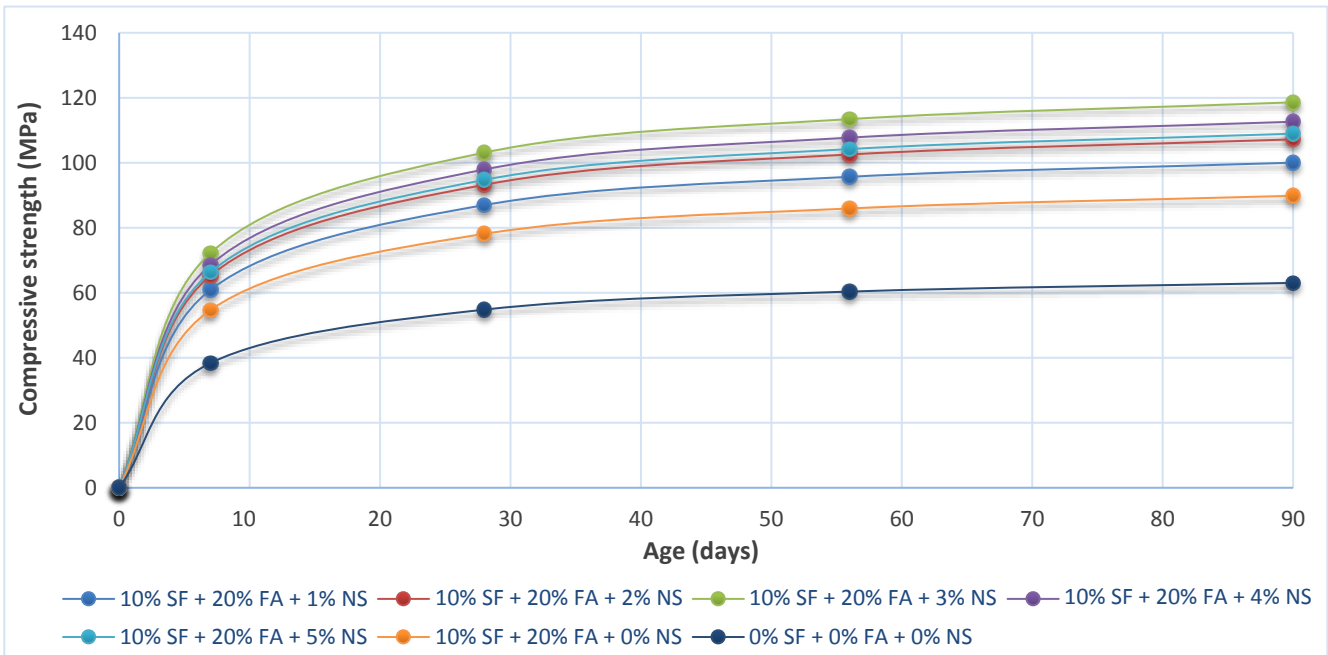


Fig. 8. Compressive strength of RPC using 10% SF + 20% FA with different ratios of nano-silica.

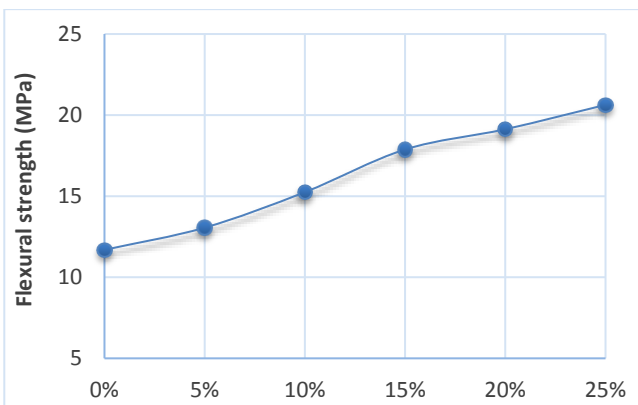


Fig. 9. Flexural strength of RPC using different ratios of silica fume.

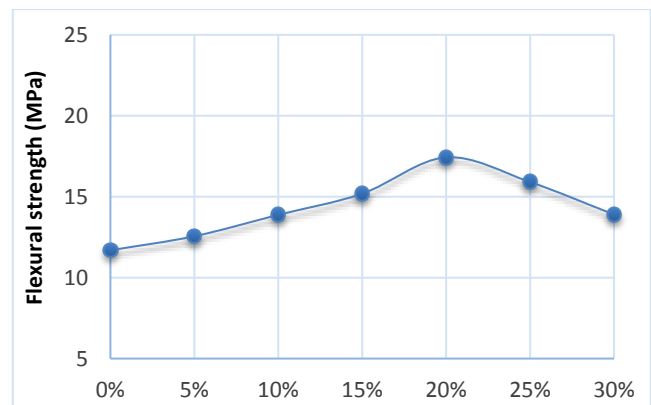


Fig. 10. Flexural strength of RPC using different ratios of fly ash.

Fig. 11 depicts flexural strength variations in concrete at 28 days as fly ash content increases from 10% to 30% while maintaining a constant 10% silica fume content. Although fly ash offers economic advantages over silica fume, it reduces the flexural resistance capacity of concrete. The 30% fly ash mixture achieved a flexural strength of 13.90 MPa, representing a 24.37% reduction compared to the 10% SF + 20% FA combination.

Comparative analysis reveals silica fume’s superior effectiveness in enhancing mixture flexural strength performance. At 28 days, concrete strength improvements of 3.98%, 9.87%, 17.71%, 9.75%, and 29.67% are attributed to the pozzolanic activity of fly ash and its interactions with SiO₂, Al₂O₃, and calcium hydroxide, which collectively promote calcium silicate hydrate formation while reducing porosity and increasing density (Malheiro et al. 2020), in addition to improving particle packing. The in-

corporation of fly ash into the cement paste also provides micro-void filling capability, resulting in increased paste density and subsequent strength development.

5.3.3. Effect of the nano-silica content

Nano-silica contents of 1%, 2%, 3%, 4%, and 5% were incorporated into mixes containing 10% SF and 20% FA to evaluate their effect on the flexural strength of RPC. Fig. 13 shows that 1% NS resulted in a 65% increase, 2% NS in a 77% increase, 3% NS in a 109% increase, 4% NS in an 86% increase, and 5% NS in a 77% increase in 28-day flexural strength compared with the control. The highest flexural strength, 24.35 MPa, was achieved with 3% NS, owing to nano-silica filling pores and promoting the formation of additional C-S-H gels (Keshavarzian et al. 2021).

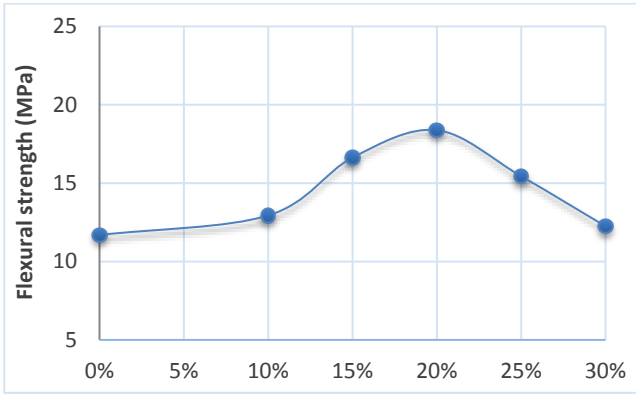


Fig. 11. Flexural strength of RPC using 10% silica fume with different ratios of fly ash.

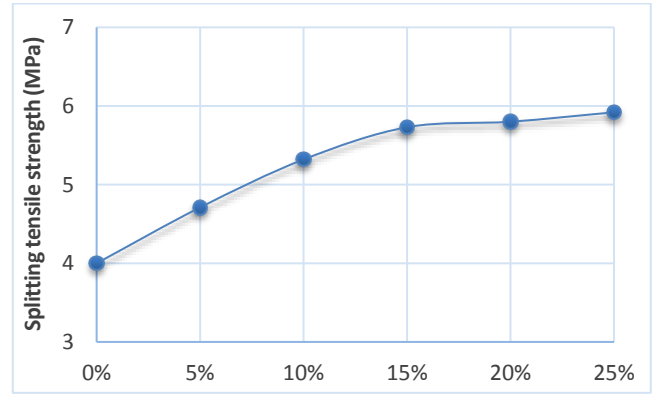


Fig. 14. Splitting Tensile strength of RPC using different ratios of silica fume.

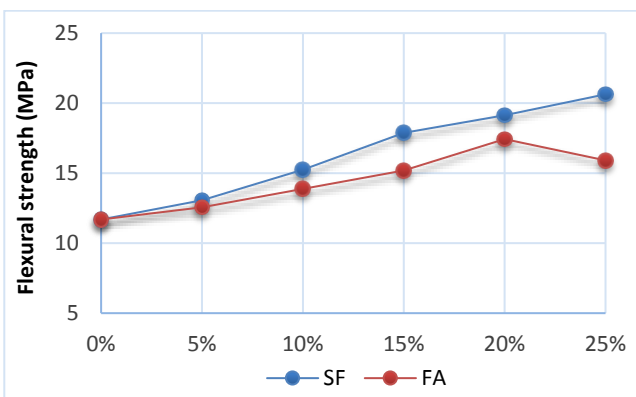


Fig. 12. Comparison between SF & FA at the same content at 28 days.

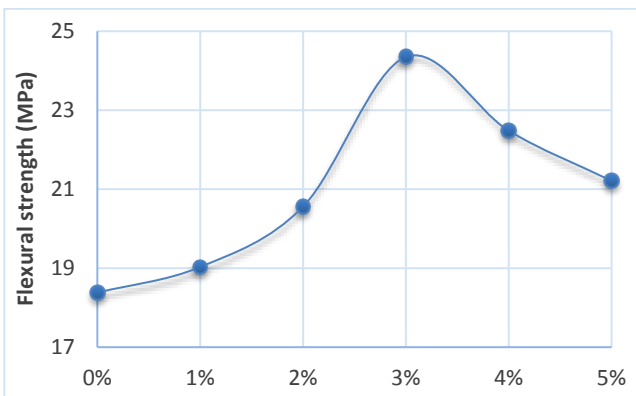


Fig. 13. Flexural strength of RPC using 10% SF + 20% FA with different ratios of nano-silica.

5.4. Splitting tensile strength of RPC

5.4.1. Effect of the silica fume content

Fig. 14 presents the splitting tensile strength of RPC mixes containing 5% to 25% silica fume at 28 days. With 25% silica fume, tensile strength increased by 17.75% to 48% compared to the control mix M00, indicating that 25% silica fume provided the best performance. This improvement is attributed to the extremely fine silica fume particles, which enhanced hydration and densification of the RPC matrix, thereby increasing strength.

5.4.2. Effect of the fly ash content

Fig. 15 shows the calculated splitting tensile strength of RPC mixes containing fly ash at 28 days, with fly ash content ranging from 5% to 30%. Compared to the control mix M00, tensile strength increased by 5%, 13%, 33.75%, 37%, 27.25%, and 13% for these respective replacement levels. The optimal performance was observed at around 20% fly ash content, where its pozzolanic activity—through reactions of SiO₂ and Al₂O₃ with calcium hydroxide (CH) to form C-S-H—produced a dense and less porous matrix, improving strength (Keshavarzian et al. 2021), alongside enhanced particle packing capacity.

Incorporating fly ash into the cement paste allowed void filling within the matrix, which increased density and consequently improved strength. However, when the fly ash content was increased from 10% to 30% while maintaining 10% silica fume, the 28-day splitting tensile strength remained nearly unchanged (Fig. 16). The strength was 4.52 MPa for the mix containing 30% fly ash, which was lower than that of the 10% SF + 20% FA combination.

When compared to fly ash, silica fume demonstrated a much greater improvement in splitting tensile strength, with increases of 12.14%, 17.70%, 7.10%, 5.84%, and 16.31% at 28 days (Fig. 17).

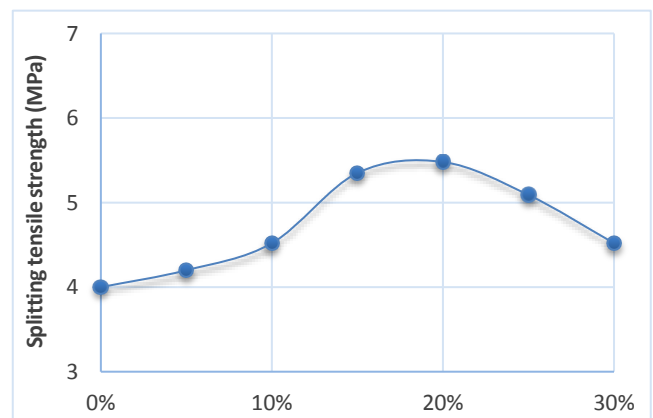


Fig. 15. Splitting tensile strength of RPC using different ratios of fly ash.

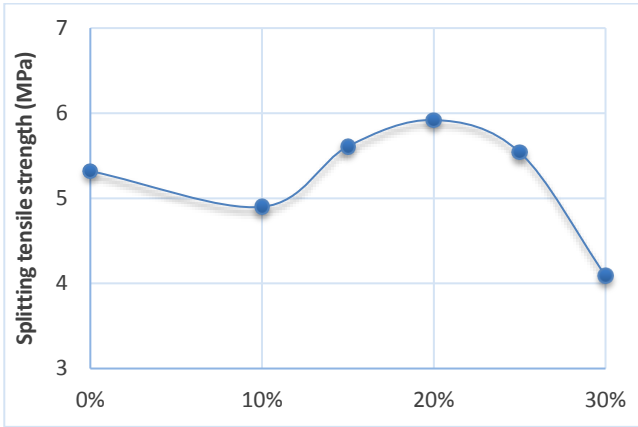


Fig. 16. Splitting tensile strength of RPC using 10% silica fume with different ratios of fly ash.

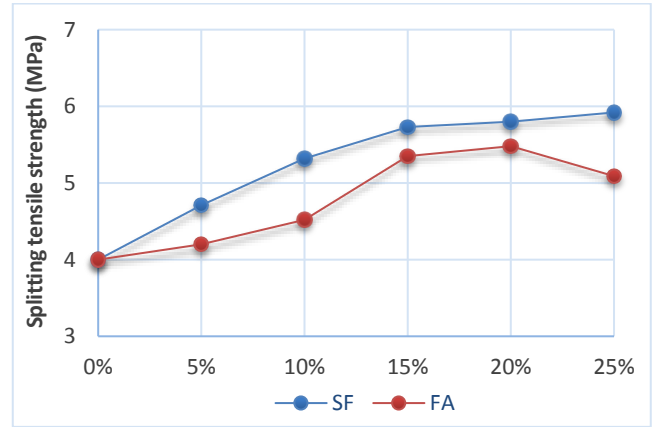


Fig. 17. Comparison between SF & FA at the same content at 28 days.

5.4.3. Effect of the nano-silica content

With 10% SF + 20% FA, compared to the control mixture, 1% NS resulted in a 76.50% increase in splitting tensile strength, 2% NS in a 122.25% increase, 3% NS in a 212% increase, 4% NS in a 155.75% increase, and 5% NS in a 127.25% increase after 28 days (Fig. 18). The mix containing 3% nano-silica achieved the highest splitting tensile strength, which was 24.35 MPa. This improvement is attributed to nano-silica filling pores and promoting the formation of additional C-S-H gels (Keshavarzian et al. 2021).

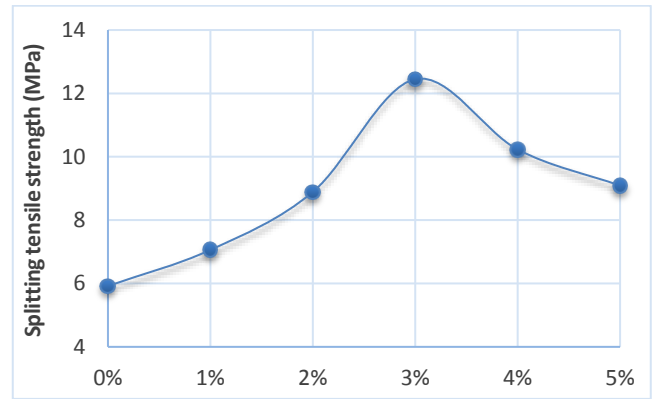


Fig. 18. Splitting tensile strength of RPC using 10% SF + 20% FA with different ratios of nano-silica.

5.5. Density of RPC

The density values shown in Fig. 19 indicate that RPC mixes containing only silica fume had densities between 2344 and 2401 kg/m³, those containing only fly ash had densities between 2375 and 2450 kg/m³, mixes with silica fume + fly ash had densities between 2436 and 2495 kg/m³, and those with silica fume + fly ash + nano-silica g had densities between 2533 and 2600 kg/m³.

When pozzolanic materials are added, they increase density because their reaction with calcium hydroxide seals small air pockets and microcracks. Due to its extremely fine and smooth particles, RPC containing nano-silica exhibits higher density than the other mixtures, according to the results.

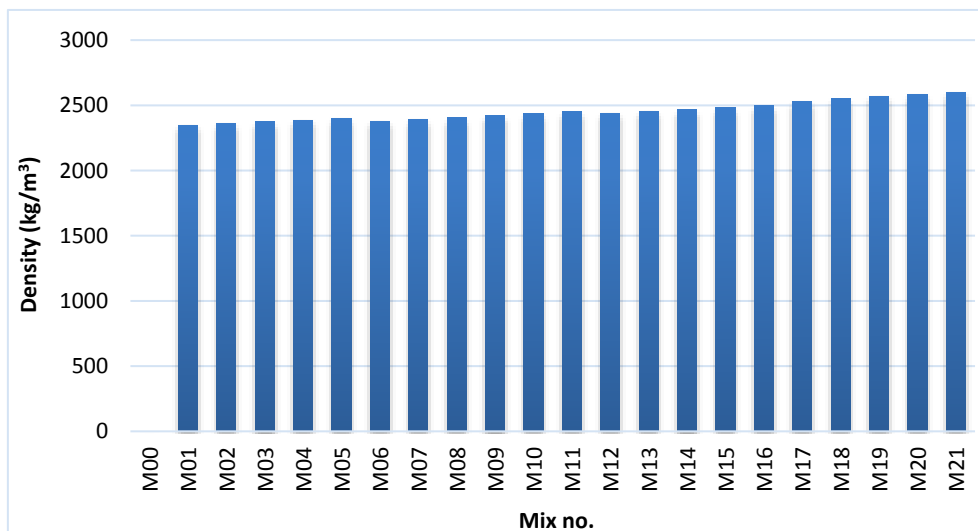


Fig. 19. Density of RPC.

6. Conclusions

Based on the research findings and analyses presented in this investigation, the following conclusions are drawn:

- Increased concentrations of silica fume, fly ash, and nano-silica reduced RPC workability, with fly ash demonstrating superior workability performance, followed by silica fume and then binary combinations.
- Nano-silica incorporation alongside fly ash and silica fume enhanced mixture density characteristics.
- Increased fineness of cementitious materials correlates with reduced workability while producing denser materials and final products.
- Increasing silica fume content within the binder system from 5% to 25% improved RPC performance in compressive, splitting tensile, and flexural strength evaluations.
- Progressive increases in fly ash content from 5% to 20% within the binder enhanced RPC compressive, tensile, and flexural strength properties. Further increases from 20% to 25% or 30% resulted in marginal reductions in compressive, splitting tensile, and flexural strength. Experimental evidence indicates an optimal fly ash content of approximately 20%.
- Fly ash substitution for silica fume in RPC provides economic benefits but compromises compressive strength performance.
- A complete 30% binder replacement with fly ash alone achieved a compressive strength of 64.88 MPa at 28 days, significantly lower than the 10% SF + 20% FA combination (72.65 MPa).
- The maximum compressive strength of 103.13 MPa at 3% nano-silica replacement resulted from effective nanoparticle packing and reduced agglomeration phenomena.
- Nano-silica produces superior strength enhancement through calcium hydroxide reactions, accelerated cement hydration, and increased calcium silicate hydrate formation within the paste matrix. Continued pozzolanic reactions generate additional strength-contributing C-S-H, improving overall mixture performance.
- Regional material sources can be employed for RPC production.
- Alternative curing methodologies, such as steam curing, are feasible.
- Hybrid fiber combinations utilizing polypropylene and steel fibers can further enhance mechanical property development.

Acknowledgements

None declared.

Funding

The authors received no financial support for the research, authorship, and/or publication of this manuscript.

Conflict of Interest

The authors declared no potential conflicts of interest with respect to the research, authorship, and/or publication of this manuscript.

Author Contributions

All of the authors made substantial contributions to conception and design, or acquisition of data, or analysis and interpretation of data; were involved in drafting the manuscript or revising it critically for important intellectual content; and gave final approval of the version to be published.

Data Availability

The datasets created and/or analyzed during the current study are not publicly available, but are available from the corresponding author upon reasonable request.

REFERENCES

- Aïtcin PC (2000). Cements of yesterday and today. *Cement and Concrete Research*, 30(9), 1349-1359.
- Aïtcin PC (2016). Supplementary cementitious materials and blended cements. In: Aïtcin PC, Flatt RJ, editors. *Science and Technology of Concrete Admixtures*. Elsevier, Amsterdam, Netherlands, 53-73.
- Albakry BA, Abbas ZK (2025). Evaluation of reactive powder concrete strength using various curing methods. *Engineering, Technology & Applied Science Research*, 15(2), 21685-21690.
- ASTM C1017 / C1017M – 13 (2013). Standard specification for chemical admixtures for use in producing flowing concrete. ASTM International, West Conshohocken, PA, USA.
- ASTM C109 / C109M – 20b (2020). Standard test method for compressive strength of hydraulic cement mortars (using 2-in. or [50-mm] cube specimens). ASTM International, West Conshohocken, PA, USA.
- ASTM C348 – 21 (2021). Standard test method for flexural strength of hydraulic-cement mortars. ASTM International, West Conshohocken, PA, USA.
- ASTM C496 / C496M – 17 (2017). Standard test method for splitting tensile strength of cylindrical concrete specimens. ASTM International, West Conshohocken, PA, USA.
- ASTM C618 – 19 (2019). Standard specification for coal fly ash and raw or calcined natural pozzolan for use in concrete. ASTM International, West Conshohocken, PA, USA.
- ASTM C642 – 13 (2013). Standard test method for density, absorption, and voids in hardened concrete. ASTM International, West Conshohocken, PA, USA.
- ASTM C1116 / C1116M – 10a (2010). Standard specification for fiber-reinforced concrete. ASTM International, West Conshohocken, PA, USA.
- ASTM C1339 / C1339M – 08 (2008). Standard specification for thin bonded overlays for bridge decks using hydraulic cement concrete. ASTM International, West Conshohocken, PA, USA.
- Bahmani H, Mostofinejad D (2022). Microstructure of ultra-high-performance concrete (UHPC) – A review study. *Journal of Building Engineering*, 50, 104118.
- Balapour M, Joshaghani A, Althoey F (2018). Nano-SiO₂ contribution to mechanical, durability, fresh and microstructural characteristics of concrete: A review. *Construction and Building Materials*, 181, 27-41.
- Chandra S, Berntsson L (1996). Use of silica fume in concrete. In: Chandra S, Berntsson L, editors. *Waste Materials Used in Concrete Manufacturing*. Elsevier, Amsterdam, Netherlands, 554-623.
- Danha LS, Khalil WI, Al-Hassani HM (2013). Mechanical properties of reactive powder concrete (RPC) with various steel fiber and silica fume contents. *Engineering and Technology Journal*, 31(16), 3090–3108.
- E.S.S. 1109 (2008). Aggregates for concrete. Egyptian Organization for Standardization and Quality (EOS), Cairo, Egypt.
- E.S.S. 4756-1 (2013). Plain and reinforced concrete – Part 1: Specifications, performance, production and conformity. Egyptian Organization for Standardization and Quality (EOS), Cairo, Egypt.

- E.S.S. 5129-1 (2006). Products and systems for the protection and repair of concrete structures – Definitions, requirements, quality control and evaluation of conformity – Part 1: Definitions. Egyptian Organization for Standardization and Quality (EOS), Cairo, Egypt.
- Ge W, Wang A, Zhang Z, Ge Y, Chen Y, Li W, Jiang H, Shuai H, Sun C, Yao S, Qiu L (2023). Study on the workability, mechanical property and water absorption of reactive powder concrete. *Case Studies in Construction Materials*, 18, e01777.
- Golewski GL (2018). An assessment of microcracks in the interfacial transition zone of durable concrete composites with fly ash additives. *Composite Structures*, 200, 515-520.
- Hefni Y, Zaher YA El, Wahab MA (2018). Influence of activation of fly ash on the mechanical properties of concrete. *Construction and Building Materials*, 172, 728-734.
- Ju Y, Tian K, Liu H, Reinhardt HW, Wang L (2017). Experimental investigation of the effect of silica fume on the thermal spalling of reactive powder concrete. *Construction and Building Materials*, 155, 571-583.
- Keshavarzian F, Saberian M, Li J (2021). Investigation on mechanical properties of steel fiber reinforced reactive powder concrete containing nano-SiO₂: An experimental and analytical study. *Journal of Building Engineering*, 44, 102601.
- Kong D, Du X, Wei S, Zhang H, Yang Y, Shah SP (2012). Influence of nano-silica agglomeration on microstructure and properties of the hardened cement-based materials. *Construction and Building Materials*, 37, 707-715.
- Kurdowski W (2014). Mineral additions for cement production. In: Kurdowski W, editor. *Cement and Concrete Chemistry*. Springer Netherlands, Dordrecht, Netherlands, 533-583.
- Malheiro R, Camões A, Meira G, Pinto J (2020). Durability of fly ash eco-friendly cement mortars in severe environment. *Procedia Manufacturing*, 46, 122-130.
- Moffatt EG, Thomas MDA, Fahim A (2017). Performance of high-volume fly ash concrete in marine environment. *Cement and Concrete Research*, 102, 127-135.
- Neville AM (2005). *Properties of Concrete* (4th and final edition). Pearson Education Limited, Harlow, England.
- Ranjan M, Kumar S, Sinha S (2024). Nanosilica's influence on concrete hydration, microstructure, and durability: A review. *Journal of Applied Engineering Sciences*, 14(2), 322-335.
- Rashad AM (2014). A comprehensive overview about the effect of nano-SiO₂ on some properties of traditional cementitious materials and alkali-activated fly ash. *Construction and Building Materials*, 52, 437-464.
- Richard P, Cheyrezy M (1995). Composition of reactive powder concretes. *Cement and Concrete Research*, 25(7), 1501-1511.
- Rupasinghe M, Mendis P, Ngo T, Nguyen TN, Sofi M (2017). Compressive strength prediction of nano-silica incorporated cement systems based on a multiscale approach. *Materials & Design*, 115, 379-392.
- Sadrekarami A (2004). Development of a light weight reactive powder concrete. *Journal of Advanced Concrete Technology*, 2(3), 409-417.
- Sarika S, Elson J (2015). A study on properties of reactive powder concrete. *International Journal of Engineering Research & Technology*, 4(11), 110-113.
- Shen M, Zhou L, Chen Z, Shen Y, Huang B, Lv J (2022). Effects of basalt powder and silica fume on ultra-high-strength cementitious matrix: A comparative study. *Case Studies in Construction Materials*, 17, e01397.
- Sultan HK, Zinkaah OH, Rasheed AA, Alridha Z, Alhawati M (2022). Producing sustainable modified reactive powder concrete using locally available materials. *Innovative Infrastructure Solutions*, 7(6), 342.
- Tan H, Yuan P, Sun D, Fan X, Wang C, Liu J (2025). Ratio of water to cement and supplementary cementitious materials on mechanical and impact resistance properties of reactive powder concrete. *Scientific Reports*, 15(1), 7480.
- Ullah R, Qiang Y, Ahmad J, Vatin NI, El-Shorbagy MA (2022). Ultra-high-performance concrete (UHPC): A state-of-the-art review. *Materials*, 15(12), 4131.
- Wang BM (2011). Influence of nano-SiO₂ on the strength of high performance concrete. *Materials Science Forum*, 686, 432-437.
- Yazıcı H, Yardımcı MY, Aydın S, Karabulut AŞ (2009). Mechanical properties of reactive powder concrete containing mineral admixtures under different curing regimes. *Construction and Building Materials*, 23(3), 1223-1231.
- Yu R, Spiesz P, Brouwers HJH (2015). Development of an eco-friendly ultra-high performance concrete (UHPC) with efficient cement and mineral admixtures uses. *Cement and Concrete Composites*, 55, 383-394.
- Zhang L, Ma N, Wang Y, Han B, Cui X, Yu X, Ou J (2016). Study on the reinforcing mechanisms of nano silica to cement-based materials with theoretical calculation and experimental evidence. *Journal of Composite Materials*, 50(29), 4135-4146.
- Zhang Y, Wang J, Wang J, Qian X (2022). Preparation, mechanics and self-sensing performance of sprayed reactive powder concrete. *Scientific Reports*, 12(1), 7787.